Inorg. Chem. **2008**, *47*, 3328−3339

Inorganic Chemistry Article

Rare-Earth Metal Complexes Supported by 1,ω-Dithiaalkanediyl-Bridged Bis(phenolato) Ligands: Synthesis, Structure, and Heteroselective Ring-Opening Polymerization of *rac*-Lactide

Haiyan Ma,[†] Thomas P. Spaniol, and Jun Okuda*

Institute of Inorganic Chemistry, RWTH Aachen University, Landoltweg 1, D-52056 Aachen, Germany

Received November 25, 2007

Monomeric yttrium and lutetium bis(phenolato) complexes [Ln(OSSO){N(SiHMe$_2$)$_2$}(THF)] (Ln = Y, Lu) were prepared from the reaction of silylamido complexes [Ln{N(SiHMe$_2$)$_2$}$_3$(THF)$_2$] with 1 equiv of tetradentate 1,ω-dithiaalkanediyl-bridged bis(phenol) (OSSO)H$_2$ **1–9** in moderate to high yields. In contrast to the rigid configuration of scandium analogues, the yttrium complexes **2b** and **3b** and the lutetium complex **3c** that contain a C$_2$ bridge between the two sulfur donors of the ligand are symmetric in solution. The monomeric nature of these complexes was indicated by an X-ray diffraction study of the yttrium complex **6b**. The yttrium center in **6b** is coordinated to the tetradentate [OSSO]-type ligand, one silylamido group and one THF ligand with the two oxygen donors of the [OSSO]-type ligand located *trans*. Corresponding bis(phenolato) silylamido complexes of larger rare-earth metals could not be obtained from similar reactions: Reaction of [La{N(SiHMe$_2$)$_2$}$_3$(THF)$_2$] with 1,2-xylylene-linked bis(phenol) gave a dinuclear lanthanum complex **6d** of the formula [La$_2$(OSSO)$_3$] with two inequivalent eight-coordinate metal centers. The yttrium and lutetium complexes efficiently initiated the ring-opening polymerization (ROP) of lactides in THF. The heteroselectivity during the ROP of *rac*-lactide was enhanced when the steric demand of the bis(phenolato) ligand was increased, either by extending the bridge length or by introducing bulky *ortho*-substituents in the phenoxy units. A C$_3$ bridge within the ligand backbone is essential to allow configurational interconversion of the active site between Λ and Δ configuration during polymerization, allowing accommodation of both enantiomers of the monomer in an alternating fashion.

Introduction

As biodegradable and biocompatible polymeric materials derived from renewable natural resources, poly(L-lactide) (PLLA) has recently attracted considerable attention.[1,2] Moreover, a PLA stereocomplex formed by blending PLLA with its enantiomer poly(D-lactide) (PDLA) shows a higher melting temperature of 230 °C as compared to that of pure PLLA or PDLA (T_m = 180 °C),[2,3] but the complicated

* To whom correspondence should be addressed. E-mail: jun.okuda@ac.rwth-aachen.de.

[†] Current address: Laboratory of Organometallic Chemistry, East China University of Science and Technology, 130 Meilong Road, 200237 Shanghai, PR China.

(1) (a) Swift, G. *Acc. Chem. Res.* **1993**, *26*, 105–110. (b) Chiellini, E.; Solaro, R. *Adv. Mater.* **1996**, *8*, 305–313. (c) Drumright, R. E.; Gruber, P. R.; Henton, D. E. *Adv. Mater.* **2000**, *12*, 1841–1846. (d) Albertsson, A.-C.; Varma, I. K. *Biomacromolecules* **2003**, *4*, 1466–1486. (e) Cabaret, O. D.; Vaca, B.-M.; Bourissou, D. *Chem. Rev.* **2004**, *104*, 6147–6176. (f) Ha, C. K.; Gardella, J. A., Jr. *Chem Rev* **2005**, *106*, 4205–4232.

(2) (a) Fukushima, K.; Kimura, Y. *Polym. Int.* **2006**, *55*, 626–642. (b) Dorgan, J. R.; Lehermeir, H.; Mang, M. *J. Polym. Environ.* **2000**, *8*, 1–9.

(3) (a) Ikada, Y.; Jamshidi, K.; Tsuji, H.; Hyon, S.-H. *Macromolecules* **1987**, *20*, 904–906. (b) Tsuji, H.; Horii, F.; Hyon, S.-H.; Ikada, Y. *Macromolecules* **1991**, *24*, 2719–2724. (c) Tsuji, H.; Hyon, S.-H.; Ikada, Y. *Macromolecules* **1991**, *24*, 5651–5656. (d) Tsuji, H.; Hyon, S.-H.; Ikada, Y. *Macromolecules* **1991**, *24*, 5657–5662. (e) Tsuji, H.; Ikada, Y. *Macromolecules* **1992**, *25*, 5719–5723.

(4) For reviews on metal initiators, see: (a) O'Keefe, B. J.; Hillmyer, M. A.; Tolman, W. B. *J. Chem. Soc., Dalton Trans.* **2001**, 2215–2224. (b) Nakano, K.; Kosaka, N.; Hiyama, T.; Nozaki, K. *Dalton Trans.* **2003**, 4039–4050. (c) Chisholm, M. H.; Zhou, Z. *J. Mater. Chem.* **2004**, *14*, 3081–3092. (d) Wu, J.; Yu, T.-L.; Chen, C.-T.; Lin, C.-C. *Coord. Chem. Rev.* **2006**, *250*, 602–626. (e) Biela, T.; Kowalski, A.; Libiszowski, J.; Duda, A. *Macromol. Symp.* **2006**, *240*, 47–55. (f) For stereoselective ROP using organocatalysts, see: Jensen, T. R.; Breyfogle, L. E.; Hillmyer, M. A.; Tolman, W. B. *Chem. Commun.* **2004**, 2504–2506. (g) Dove, A. P.; Li, H.; Pratt, R. C.; Lohmeijer, B. G.; Culkin, D. A.; Waymouth, R. M.; Hedrick, J. L. *Chem. Commun.* **2006**, 2881–2883. (h) For a review on organocatalysts for ROP, see: Kamber, N. E.; Jeong, W.; Waymouth, R. M.; Pratt, R. C.; Lohmeijer, B. G. G.; Hedrick, J. L. *Chem. Rev.* **2007**, *107*, 5813–5840.

10.1021/ic702312b CCC: $40.75

Published on Web 03/04/2008

stereocomplexation processes restrict practical application.[3] Metal-catalyzed stereoselective ring-opening polymerization (ROP) of lactides is expected to provide new methods to control the microstructure of PLA formed during polymerization.[4] So far, PLAs with various microstructures ranging from isotactic[5,6] and heterotactic[7–12] to syndiotactic[13] can be obtained from metal-initiated stereoselective ROP of *rac*-lactide and *meso*-lactide. Aluminum complexes with chiral-bridged bis(iminophenolato) ligands have been reported to polymerize *rac*-LA to isotactic or stereoblock/stereogradient PLA[5a–h] and to polymerize *meso*-LA to syndiotactic PLA via enantiomorphic site control.[13a] Achiral aluminum bis(iminophenolato) or bis(aminophenolato) complexes produce isotactic[5i–q] or heterotactic PLA[7] from *rac*-LA via a chain-end control mechanism. Zinc,[8] magnesium,[9] calcium,[10] and rare-earth metal[11] complexes are highly active for ROP of *rac*-LA, in some cases showing significant preference for heterotactic dyad enchainment. Although the nature of the metal center and the ancillary ligand sphere critically influence the polymerization behavior,[5–14] the factors that govern the stereocontrol during the ROP of lactides are still not well understood. It is believed that a proper design of the ancillary ligand will eventually allow fine-tuning of the stereoselectivity. Recently, we have introduced a series of 1,ω-dithiaalkanediyl-bridged bis(phenol)s (Scheme 1) as ancillary ligands for scandium complexes (Scheme 2).[15] By variation of the ligand architecture, we have obtained moderate to high heteroselectivity for the ROP of *rac*-LA.[11d] A dynamic monomer recognition step based on the ancillary ligand's fluxionality was suggested to be responsible for the high heteroselectivity. In order to further investigate the influence of this ligand framework on the polymerization behavior of the resulting complexes in the ROP of lactides, we have now extended this ligand system to other rare-earth metals.

Results and Discussion

Synthesis. Similar to the previously reported yttrium complexes **1b** and **5b**,[15a] complex **2b** was synthesized by amine elimination reaction of yttrium silylamide [$Y\{N(SiHMe_2)_2\}_3(THF)_2$] and 1 equiv of 1,4-dithiabutanediyl-2,2′-bis{4,6-di(2-phenyl-2-propyl)phenol} (etccpH_2, **2**) in toluene at 50 °C (Scheme 2). Due to the bulky cumyl substituent in the bis(phenol) framework, complete complexation was reached only after 8 days. Workup of the reaction mixture afforded analytically pure **2b** as colorless microcrystals, which were characterized by NMR spectroscopy and elemental analysis. Attempts to obtain single

(5) For aluminum complexes showing isotactic selectivity, see: (a) Spassky, N.; Wisnieski, M.; Pluta, C.; Le Borgne, A. *Macromol. Chem. Phys.* **1996**, *197*, 2627–2637. (b) Radano, C. P.; Baker, G. L.; Smith, M. R., III *J. Am. Chem. Soc.* **2000**, *122*, 1552–1553. (c) Ovitt, T. M.; Coates, G. W. *J. Polym. Sci., A: Polym. Chem.* **2000**, *38*, 4686–4692. (d) Ovitt, T. M.; Coates, G. W. *J. Am. Chem. Soc.* **2002**, *124*, 1316–1326. (e) Majerska, K.; Duda, A. *J. Am. Chem. Soc.* **2004**, *126*, 1026–1027. (f) Zhong, Z.; Dijkstra, P. J.; Feijen, J. *Angew. Chem.* **2002**, *114*, 4692–4695. (g) Zhong, Z.; Dijkstra, P. J.; Feijen, J. *J. Am. Chem. Soc.* **2003**, *125*, 11291–11298. (h) Chisholm, M. H.; Patmore, N. J.; Zhou, Z. *Chem. Commun.* **2005**, 127–129. (i) Nomura, N.; Ishii, R.; Akakura, M.; Aoi, K. *J. Am. Chem. Soc.* **2002**, *124*, 5938–5939. (j) Tang, Z.; Chen, X.; Pang, X.; Yang, Y.; Zhang, X.; Jing, X. *Biomacromolecules* **2004**, *5*, 965–970. (k) Tang, Z.; Chen, X.; Yang, Y.; Pang, X.; Sun, J.; Zhuang, X.; Jing, X. *J. Polym. Sci., A: Polym. Chem.* **2004**, *42*, 5974–5982. (l) Tang, Z.; Yang, Y.; Pang, X.; Hu, J.; Chen, X.; Hu, N.; Jing, X. *J. Appl. Polym. Sci.* **2005**, *98*, 102–108. (m) Tang, Z.; Pang, X.; Sun, J.; Du, H.; Chen, X.; Wang, X.; Jing, X. *J. Polym. Sci., A: Polym. Chem.* **2006**, *44*, 4932–4938. (n) Du, H.; Pang, X.; Yu, H.; Zhuang, X.; Chen, X.; Cui, D.; Wang, X.; Jing, X. *Macromolecules* **2007**, *40*, 1904–1913. (o) Pang, X.; Du, H.; Chen, X.; Zhuang, X.; Cui, D.; Jing, X. *J.Polym. Sci., A: Polym. Chem.* **2005**, *43*, 6605–6612. (p) Tang, Z.; Gibson, V. C. *Eur. Polym. J.* **2007**, *43*, 150–155. (q) Nomura, N.; Ishii, R.; Yamamoto, Y.; Kondo, T. *Chem.—Eur. J.* **2007**, *13*, 4433–4451.

(6) (a) For other metal complexes showing isotactic preference, see: Wu, J.-C.; Huang, B.-H.; Hsueh, M.-L.; Lai, S.-L.; Lin, C.-C. *Polymer* **2005**, *46*, 9784–9792. (b) Jensen, T. R.; Breyfogle, L. E.; Hillmyer, M. A.; Tolman, W. B. *Chem. Commun.* **2004**, 2504–2505. (c) Wang, X.; Liao, K.; Quan, D.; Wu, Q. *Macromolecules* **2005**, *38*, 4611–4617. (d) Chmura, A. J.; Davidson, M. G.; Jones, M. D.; Lunn, M. D.; Mahon, M. F.; Johnson, A. F.; Khunkamchoo, P.; Roberts, S. L.; Wong, S. S. F. *Macromolecules* **2006**, *39*, 7250–7257. (e) Schuez, S. A.; Silvernail, C. M.; Incarvito, C. D.; Rheingold, A. L.; Clark, J. L.; Day, V. W.; Belot, J. A. *Inorg. Chem.* **2004**, *43*, 6203–6214. (f) Heck, R.; Schulz, E.; Collin, J.; Carpentier, J.-F. *J. Mol. Catal. A: Chem.* **2007**, *268*, 163–168.

(7) For aluminium complexes showing heterotactic preference, see: (a) Gibson, V. C.; Hormnirun, P.; Marshall, E. L. *Polym. Prep.* **2004**, *45*, 474–475. (b) Hormnirun, P.; Marshall, E. L.; Gibson, V. C.; White, A. J. P.; Williams, D. J. *J. Am. Chem. Soc.* **2004**, *126*, 2688–2689.

(8) For zinc complexes showing heterotactic preference, see: (a) Cheng, M.; Attygalle, A. B.; Lobkovsky, E. B.; Coates, G. W. *J. Am. Chem. Soc.* **1999**, *121*, 11583–11584. (b) Chamberlain, B. M.; Cheng, M.; Moore, D. R.; Ovitt, T. M.; Lobkovsky, E. B.; Coates, G. W. *J. Am. Chem. Soc.* **2001**, *123*, 3229–3238. (c) Chen, H.-Y.; Huang, B.-H.; Lin, C.-C. *Macromolecules* **2005**, *38*, 5400–5405. (d) Chen, H.-Y.; Tang, H.-Y.; Lin, C.-C. *Macromolecules* **2006**, *39*, 3745–3752. (e) Chisholm, M. H.; Lin, C.-C.; Gallucci, J. C.; Ko, B.-T. *Dalton Trans.* **2003**, 406–412.

(9) For magnesium complexes showing heterotactic preference, see: (a) Chisholm, M. H.; Gallucci, J. C.; Phomphrai, K. *Inorg. Chem.* **2005**, *44*, 8004–8010. (b) Chivers, T.; Fedorchuk, C.; Parvez, M. *Organometallics* **2005**, *24*, 580–586.

(10) For calcium complexes showing heterotactic preference, see: (a) Chisholm, M. H.; Gallucci, J.; Phomphrai, K. *Chem. Commun.* **2003**, 48–49. (b) Chisholm, M. H.; Gallucci, J.; Phomphrai, K. *Inorg. Chem.* **2004**, *43*, 6717–6725.

(11) For rare-earth metal complexes showing heterotactic selectivity, see: (a) Cai, C.-X.; Amgoune, A.; Lehmann, C. W.; Carpentier, J.-F. *Chem. Commun.* **2004**, 330–331. (b) Amgoune, A.; Thomas, C. M.; Roisnel, T.; Carpentier, J.-F. *Chem.—Eur. J.* **2006**, *12*, 169–179. (c) Bonnet, F.; Cowley, A. R.; Mountford, P. *Inorg. Chem.* **2005**, *44*, 9046–9055. (d) Ma, H.; Spaniol, T. P.; Okuda, J. *Angew. Chem., Int. Ed.* **2006**, *45*, 7818–7821. (e) Liu, X.; Shang, X.; Tang, T.; Hu, N.; Pei, F.; Cui, D.; Chen, X.; Jing, X. *Organometallics* **2007**, *26*, 2747–2757. (f) Amgoune, A.; Thomas, C. M.; Carpentier, J.-F. *Macromol. Rapid Commun.* **2007**, *28*, 693–697. (g) For an early example, see: McLain, S. J.; Ford, T. M.; Drysdale, N. E. *Polym. Prepr.* **1992**, *33*, 463–464.

(12) For other metal complexes showing heterotactic preference, see: (a) Russel, S. K.; Gamble, C. L.; Gibbins, K. J.; Juhl, K. C. S.; Mitchell, W. S., III; Tumas, A. J.; Hofmeister, G. E. *Macromolecules* **2005**, *38*, 10336–10340. (b) Ejfler, J.; Kobylka, M.; Jerzykiewicz, L. B.; Sobota, P. *J. Mol. Catal. A: Chem.* **2006**, *257*, 105–111. (c) Atkinson, R. C. J.; Gerry, K.; Gibson, V. C.; Long, N. J.; Marshall, E. L.; West, L. J. *Organometallics* **2007**, *26*, 316–320. (d) Kim, Y.; Jnaneshwara, G. K.; Verkade, J. G. *Inorg. Chem.* **2003**, *42*, 1437–1447. (e) Dove, A. P.; Gibson, V. C.; Marshall, E. L.; White, A. J. P.; Williams, D. J. *Chem. Commun.* **2001**, 283–284. (f) Dove, A. P.; Gibson, V. C.; Marshall, E. L.; Rzepa, H. S.; White, A. J. P.; Williams, D. J. *J. Am. Chem. Soc.* **2006**, *128*, 9834–9843. (g) Chmura, A. J.; Chuck, C. J.; Davidson, M. G.; Jones, M. D.; Lunn, M. D.; Bull, S. D.; Mahon, M. F. *Angew. Chem., Int. Ed.* **2007**, *46*, 2280–2283.

(13) For metal complexes showing stereoselectivity for *meso*-lactide, see: (a) Ovitt, T. M.; Coates, G. W. *J. Am. Chem. Soc.* **1999**, *121*, 4072–4073. (b) Chisholm, M. H.; Eilerts, N. W.; Huffman, J. C.; Iyer, S. S.; Pacold, M.; Phomphrai, K. *J. Am. Chem. Soc.* **2000**, *122*, 11845–11854.

(14) Marshall, E. L.; Gibson, V. C.; Rzepa, H. S. *J. Am. Chem. Soc.* **2005**, *127*, 6048–6051.

(15) (a) Ma, H.; Spaniol, T. P.; Okuda, J. *Dalton Trans.* **2003**, 4770–4780. (b) Ma, H.; Okuda, J. *Macromolecules* **2005**, *38*, 2665–2673.

Scheme 1. Linked Bis(phenol)s $(OSSO)H_2$, **1**−**9** (ada = 1-adamantyl)

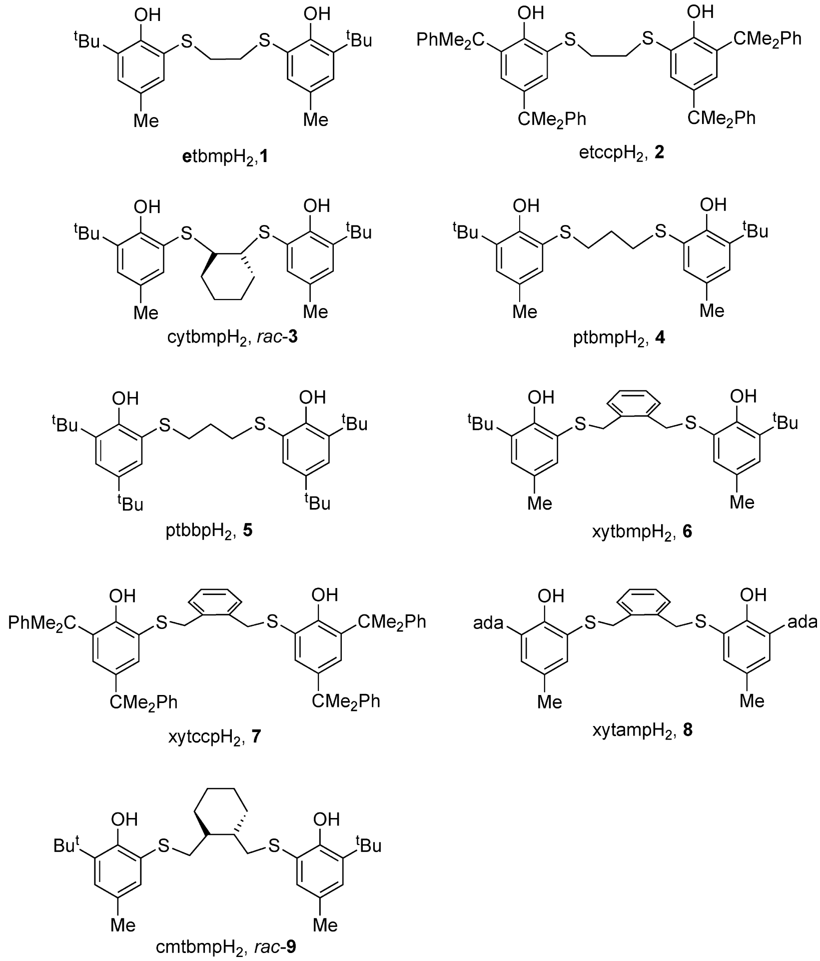

Scheme 2

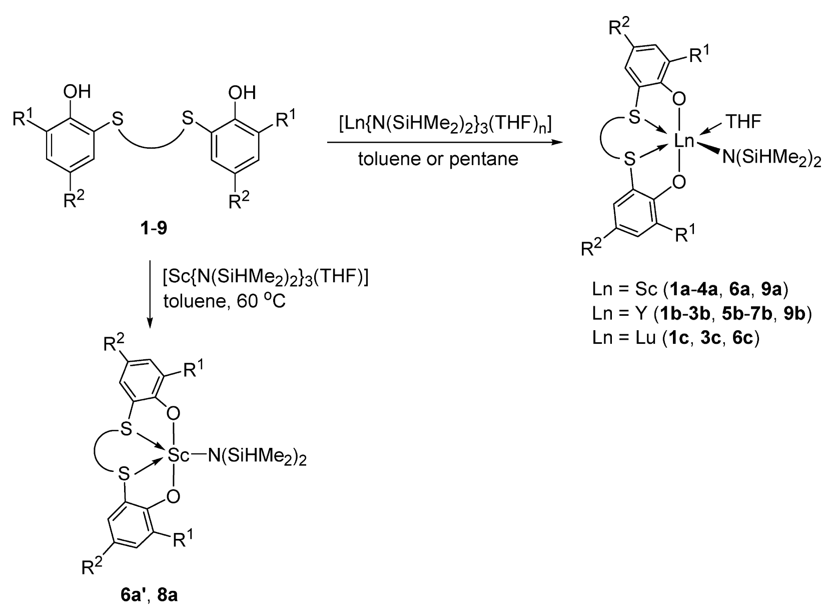

crystals by recrystallization from aliphatic hydrocarbons led to partial decomposition of the product. Similarly, **7b** was isolated in quantitative yield by simple evaporation of all volatiles from the reaction mixture of $[Y\{N(SiHMe_2)_2\}_3(THF)_2]$ with *ortho*-xylylenedithiobis{4,6-di(2-phenyl-2-propyl)phenol} ($xytccpH_2$, **7**).

When $[Y\{N(SiHMe_2)_2\}_3(THF)_2]$ was treated with *rac*-(2,3-*trans*-butanediyl-1,4-dithiabutanediyl)-2,2′-bis{6-*tert*-butyl-4-methylphenol} ($cytbmpH_2$, *rac*-**3**), *ortho*-xylylenedithiobis(6-*tert*-butyl-4-methylphenol) ($xytbmpH_2$, **6**), or *rac*-(3,4-*trans*-butanediyl-1,6-dithiahexanediyl)-2,2′-bis(6-*tert*-butyl-4-methylphenol) ($cmtbmpH_2$, *rac*-**9**) in *n*-pentane at ambient

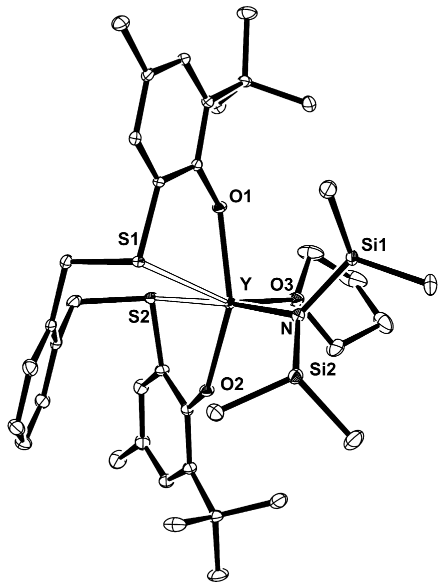

Figure 1. ORTEP diagram of the molecular structure of [Y(xytbmp){N(SiHMe$_2$)$_2$}(THF)] (**6b**). Thermal ellipsoids are drawn at the 30% probability level. Hydrogen atoms are omitted for clarity.

temperature, colorless crystals of **3b**, **6b**, and **9b** were isolated in moderate to good yields after recrystallization from aliphatic hydrocarbons. Lutetium complexes **3c** and **6c** were synthesized in good yields by reacting [Lu{N(SiHMe$_2$)$_2$}$_3$(THF)$_2$] with the corresponding bis(phenol), following a procedure analogous to that to prepare the yttrium complexes.

According to its ^{1}H NMR spectrum in C_6D_6, the solid obtained by simple evaporation of the reaction mixture of [Y{N(SiHMe$_2$)$_2$}$_3$(THF)$_2$] and *ortho*-xylylenedithiobis(6-adamantyl-4-methylphenol) (xytampH$_2$, **8**) contains one bis(phenolato) ligand, one bis(dimethylsilyl)amido group, and one-half of an equivalent of THF ligand. Attempts to isolate pure product by recrystallization of the residue from aliphatic hydrocarbons were unsuccessful. It seems that the incorporated THF ligand is highly labile, leading to decomposition of the product during solvent extraction.

Spectroscopic data and elemental analyses of all the yttrium and lutetium complexes are consistent with the structure consisting of one bis(phenolato) ligand, one bis(dimethylsilyl)amido group, and one coordinated THF molecule at the metal center. Their monomeric nature was further confirmed by an X-ray diffraction study on a single crystal of the yttrium complex **6b** (Figure 1). In contrast to the rigid C_1 configuration of the scandium complexes with a C_2 bridge,[11d,15a] complexes **2b**, **3b**, and **3c** possess high symmetry in solution. The fast dissociation of THF on the NMR time scale leads to a pseudo-five-coordinated environment around the metal center with either C_2-(trigonal bipyramidal) or C_s-symmetry (square pyramidal).[15a,16] This renders both phenyl moieties of the same ligand chemically equivalent, and only one set of signals is observed in the ^{1}H NMR spectra. Two sets of doubled signals are displayed for the SiMe protons in complexes **3b**, **3c**, and **9b**, as the chiral *trans*-cyclohexanediyl backbone of the bis(phenolato) ligands renders them diastereotopic.

The 1,ω-dithiaalkanediyl-bridged bis(phenol)s were also tested to coordinate at other rare-earth metals. The NMR scale reaction of 1 equiv of bis(phenol) **6** with samarium silylamide [Sm{N(SiHMe$_2$)$_2$}$_3$(THF)$_2$] in C_6D_6 showed the formation of the expected product, but no product was obtained after workup using *n*-hexane. Similar NMR scale reaction with [La{N(SiHMe$_2$)$_2$}$_3$(THF)$_2$] also suggested the formation of [La(xytbmp){N(SiHMe$_2$)$_2$}]. On a synthetic scale, recrystallization from toluene/pentane only gave a small amount of colorless prisms, which show unidentifiable signals in the ^{1}H NMR spectrum in pure C_6D_6. When a drop of THF-d_8 is added to C_6D_6, this compound shows two sets of signals in a 2:1 ratio for the bis(phenolato) ligand and resonances for the silylamido group are absent.[17] A single-crystal X-ray diffraction study revealed a dinuclear structure that contains three bis(phenolato) ligands, [La$_2$(xytbmp)$_3$] (**6d**) (Scheme 3 and Figure 2). This product could be obtained in better yield by reacting 2 equiv of [La{N(SiHMe$_2$)$_2$}$_3$(THF)$_2$] with 3 equiv of bis(phenol) ligand. Satisfactory elemental analysis could not be obtained due to the presence of other unidentifiable substances. Treatment of **6d** with [La{N(SiHMe$_2$)$_2$}$_3$(THF)$_2$] in C_6D_6 led to the formation of [La(xytbmp){N(SiHMe$_2$)$_2$}] but was accompanied by significant decomposition as indicated by formation of HN(SiHMe$_2$)$_2$.

Crystal Structure of 6b and 6d. Single crystals of **6b** and **6d** suitable for X-ray diffraction were obtained by slightly cooling the saturated *n*-hexane solution or toluene/pentane mixture. Crystallographic data and results of the refinements are summarized in Table 1, and selected bond lengths and angles are listed in Tables 2 and 3.

As depicted in Figure 1, the yttrium center in **6b** is six-coordinate, ligated to the tetradentate bis(phenolato) [OSSO]-type ligand, one bis(dimethylsilyl)amido group, and one coordinated THF ligand and adopts a distorted octahedral coordination geometry. The silylamido ligand is located *cis* to THF and *trans* to one of the sulfur atoms; the two oxygen donors of the bis(phenolato) ligand are arranged *trans* to each other, as indicated by the corresponding angles N−Y−O3 98.13(6), N−Y−S2 174.73(4), and O1−Y−O2 148.64(5)°. Compared to the scandium analogue **6a**,[11d] all of these angles are slightly decreased, possibly due to the larger radius of the yttrium atom. Both enantiomers of the C_1-symmetric molecule are found in the centrosymmetric crystal structure. The Y−O(ligand) bond lengths of 2.1609(14) and 2.1682(14) Å in **6b** fall into the range of terminal Y−O bond lengths in

(16) (a) Aubrecht, K. B.; Chang, K.; Hillmyer, M. A.; Tolman, W. B. *J. Polym. Sci., A: Polym. Chem.* **2001**, *39*, 284–293. (b) Arndt, S.; Voth, P.; Spaniol, T. P.; Okuda, J. *Organometallics* **2000**, *19*, 4690–4700. (c) Gountchev, T. I.; Tilley, T. D. *Organometallics* **1999**, *18*, 5661–5667.

(17) [La$_2$(xytbmp)$_3$], **6d**: ^{1}H NMR (C_6D_6 with a small amount of THF-d_8, 200 MHz): δ 7.39 (d, 4H, $^4J_{HH}$ = 1.8 Hz, 5-*H*), 7.21 (4, 2H, $^4J_{HH}$ = 1.8 Hz, 3-*H*), 7.12 (m, 2H, overlapped), 7.06 (m, 2H), 7.00 (m, 4H, Ar-*H*), 6.85 (m, 2H, Ar-*H*), 6.67 (m, 4H, Ar-*H*), 6.35 (m, 2H, Ar-*H*), 3.98 (s, 8H, SC*H*$_2$), 3.76 (s, 4H, SC*H*$_2$), 2.32 (s, 12H, 4-C*H*$_3$), 2.10 (s, 6H, 4-C*H*$_3$), 1.69 (s, 36H, 6-C(C*H*$_3$)$_3$), 1.65 (s, 18H, 6-C(C*H*$_3$)$_3$).

Scheme 3

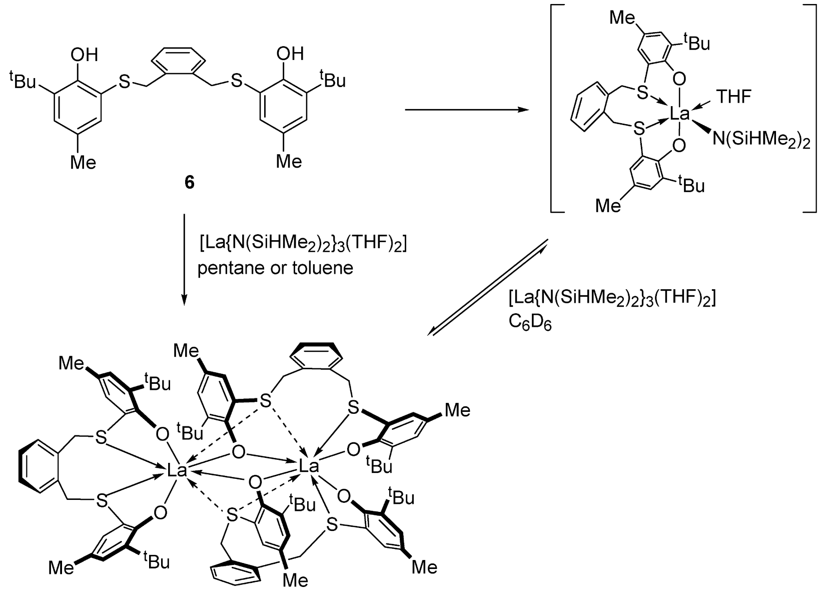

6d

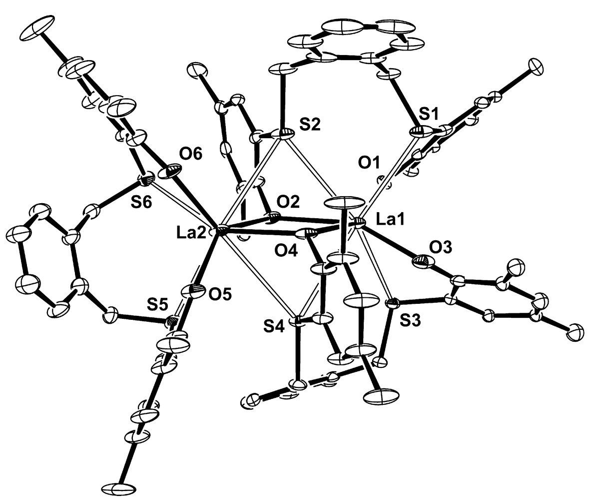

Figure 2. ORTEP diagram of the molecular structure of $[La_2(xytbmp)_3]$ (**6d**). Thermal ellipsoids are drawn at the 30% probability level. Hydrogen atoms, methyl groups of the *tert*-butyl substituents (as well as the solvent molecules toluene and pentane) are omitted for clarity.

octahedral complexes (2.104–2.177 Å)[18] and are slightly longer than those in five-coordinate complexes, such as $[Y\{O\text{-SiHMe}_2\text{-calix[4]arene}\}(THF)]_2$ (2.061–2.069 Å),[19] $[Y(1,3\text{-}(SiMe_3)_2\text{-}2\text{-Ph-}\beta\text{-diketiminato})_2(OC_6H_2{}^tBu_2\text{-}2,6\text{-Me-}4)]$ (2.075(2) Å),[16a] and $[Y\{2\text{-}(Et_2NCH_2CH_2)_2NCH_2\text{-}4,6\text{-}{}^tBu_2\text{-}C_6H_2O\}\{N(SiHMe_2)_2\}_2]$ (2.055(5) Å).[20] In contrast to the yttrium complex **5b** (Y−O(ligand) = 2.132(5) and 2.151(5) Å; Y−O(THF) = 2.382(5) Å), which has a trigonal-prismatic coordination geometry and *cis*-oriented oxygen donors of the bis(phenolato) ligand,[15a] complex **6b** possesses slightly longer Y−O(ligand) bond lengths and a shorter Y−O(THF) bond length of 2.3069(16) Å. Nevertheless, both the Y−N bond lengths in **5b** and **6b** are comparable, matching the values (2.229(4)−2.276(4) Å) found for the corresponding precursor.[21] The Y−S1 and Y−S2 bond lengths in **6b** differ from each other by about 0.09 Å, with an elongated Y−S2 bond *trans* to the $N(SiHMe_2)_2$ moiety. This can be explained

Table 1. Crystallographic Data for **6b** and **6d**

	6b	**6d**
formula	$C_{38}H_{58}NO_3S_2Si_2Y$	$C_{103}H_{126}La_2O_6S_6$
M_r	786.10	1930.22
temperature/K	130(2)	120(2)
crystal size/mm	0.80 × 0.70 × 0.60	0.42 × 0.16 × 0.15
crystal system	monoclinic	monoclinic
space group	$P2_1/n$	$C2/c$
a/Å	9.975(3)	48.696(3)
b/Å	23.333(8)	20.2759(13)
c/Å	17.589(6)	21.3906(13)
β/deg	98.237(7)	104.676(3)
U/Å^3	4052(2)	20431(2)
Z	4	8
D_c/g cm^{-3}	1.289	1.255
μ/mm^{-1}	1.636	0.997
F(000)	1664	8016
θ range/deg	2.10–28.37	0.86–26.14
data collected (hkl)	±13, −31 to 26, −20 to 23	−58 to 60, ± 25, ± 26
no. of reflection collected	27108	101915
no. of independent reflns	10032	20279
R_{int}	0.0433	0.0903
final R_1, wR_2 [$I > 2\sigma(I)$]	0.0362, 0.0896	0.0889, 0.1853
R_1, wR_2 (all data)	0.0495, 0.0954	0.1327, 0.2019
goodness of fit on F^2	1.017	1.161
$\Delta\rho_{max,min}$/e Å^{-3}	0.874, −0.684	1.546, −0.950

(18) (a) Runte, O.; Priermeier, T.; Anwander, R. *Chem. Commun.* **1996**, 1385–1386. (b) Lara-Sanchez, A.; Rodriguez, A.; Hughes, D. L.; Schormann, M.; Bochmann, M. *J. Organomet. Chem.* **2002**, *663*, 63–69. (c) Emslie, D. J. H.; Piers, W. E.; Parvez, M.; McDonal, R. *Organometallics* **2002**, *21*, 4226–4240. (d) Lara-Sanchez, A.; Rodriguez, A.; Hughes, D. L.; Schormann, M.; Bochmann, M. *J. Organomet. Chem.* **2002**, *663*, 63–69. (e) Boyd, C. L.; Toupance, T.; Tyrrell, B. R.; Ward, B. D.; Wilson, C. R.; Cowley, A. R.; Mountford, P. *Organometallics* **2005**, *24*, 309–330. (f) Marinescu, S. C.; Agapie, T.; Day, M. W.; Bercaw, J. E. *Organometallics* **2007**, *26*, 1178–1190.

(19) Anwander, R.; Eppinger, J.; Nagl, I.; Scherer, W.; Tafipolsky, M.; Sirsch, P. *Inorg. Chem.* **2000**, *39*, 4713–4720.

(20) Westmoreland, I.; Arnold, J. *Dalton Trans.* **2006**, 4155–4163.

(21) Anwander, R.; Runte, O.; Eppinger, J.; Gerstberger, G.; Herdtweck, E.; Spiegler, M. *J. Chem. Soc., Dalton Trans.* **1998**, 847–858.

Table 2. Selected Bond Lengths (Å) and Angles (deg) in **6b**

Y−N	2.2345(17)	Y−S1	2.8831(10)
Y−O1	2.1682(14)	Y−S2	2.9736(9)
Y−O2	2.1609(14)	N−Si1	1.7098(18)
Y−O3	2.3069(16)	N−Si2	1.7092(18)
Y···Si1	3.3684(10)	Y···Si2	3.4809(12)
O1−Y−S1	69.72(4)	N−Y−O1	103.41(6)
O2−Y−S1	109.82(5)	N−Y−O2	107.95(6)
O3−Y−S1	158.85(4)	N−Y−O3	98.13(6)
O1−Y−S2	81.01(4)	N−Y−S1	89.67(5)
O2−Y−S2	67.69(4)	N−Y−S2	174.73(4)
O3−Y−S2	78.90(4)	Y−N−Si1	116.67(9)
S1−Y−S2	94.619(19)	Y−N−Si2	123.38(9)
O1−Y−O2	148.64(5)	Si1−N−Si2	119.65(10)
O1−Y−O3	89.30(6)	O2−Y−O3	86.53(6)

Table 3. Selected Bond Lengths (Å) and Angles (deg) in **6d**

La1−O1	2.273(5)	La1−S1	3.187(2)
La1−O2	2.492(6)	La1−S2	3.325(2)
La1−O3	2.242(7)	La1−S3	3.177(2)
La1−O4	2.530(5)	La1−S4	3.302(2)
La2−O2	2.527(5)	La2−S2	3.254(2)
La2−O4	2.473(6)	La2−S4	3.358(2)
La2−O5	2.252(6)	La2−S5	3.162(3)
La2−O6	2.261(6)	La2−S6	3.215(3)
La1−La2	4.0705(8)		
O1−La1−S1	62.92(13)	O3−La1−S1	81.63(16)
O1−La1−S2	91.80(14)	O3−La1−S2	142.20(17)
O1−La1−S3	78.62(14)	O3−La1−S3	63.21(17)
O1−La1−S4	145.61(13)	O3−La1−S4	85.76(17)
O2−La1−S1	123.14(13)	O4−La1−S1	102.72(13)
O2−La1−S2	54.16(13)	O4−La1−S2	62.51(12)
O2−La1−S3	103.41(12)	O4−La1−S3	126.25(12)
O2−La1−S4	68.96(13)	O4−La1−S4	53.42(12)
O1−La1−O2	97.78(18)	S1−La1−S2	72.53(7)
O1−La1−O3	100.6(2)	S1−La1−S3	121.43(6)
O1−La1−O4	154.01(18)	S1−La1−S4	151.01(6)
O2−La1−O3	154.2(2)	S2−La1−S3	154.57(6)
O2−La1−O4	71.14(18)	S2−La1−S4	103.74(6)
O3−La1−O4	98.3(2)	S3−La1−S4	74.28(5)
O5−La2−S2	150.06(19)	O2−La2−S2	55.08(13)
O5−La2−S4	75.07(16)	O2−La2−S4	67.64(12)
O5−La2−S5	62.94(18)	O2−La2−S5	91.55(13)
O5−La2−S6	121.07(19)	O2−La2−S6	79.67(13)
O6−La2−S2	78.62(17)	O4−La2−S2	64.16(13)
O6−La2−S4	164.56(17)	O4−La2−S4	52.79(12)
O6−La2−S5	119.81(19)	O4−La2−S5	119.06(13)
O6−La2−S6	62.61(18)	O4−La2−S6	144.21(13)
O2−La2−O4	71.51(18)	S2−La2−S4	104.05(6)
O2−La2−O5	141.12(19)	S2−La2−S5	145.06(6)
O2−La2−O6	123.81(19)	S2−La2−S6	82.14(7)
O4−La2−O5	94.7(2)	S4−La2−S5	66.48(6)
O4−La2−O6	117.9(2)	S4−La2−S6	132.62(6)
O5−La2−O6	94.9(2)	S5−La2−S6	81.72(6)
La1−O2−La2	108.4(2)	La1−O4−La2	108.9(2)

by the stronger electron-donating ability of the silylamido group that weakens the opposite Y−S2 bond. Further features such as a Si1−N−Si2 angle of 119.65(10)° that is nearly ideal for sp^2 hybridization and the absence of Y· Si and Y·H contacts exclude a β(Si−H) agostic interaction in complex **6b**. This is further supported by the spectroscopic data of **6b**, where the septet signal of Si *H* at 5.00 ppm is virtually not shifted compared to the chemical shift of 4.99 ppm in $[Y\{N(SiHMe_2)_2\}_3(THF)_2]$.[21]

The lanthanum complex **6d** contains two unsymmetrically coordinated lanthanum centers (Figure 2) and can be thought of consisting of a cationic fragment $[Ln(OSSO)]^+$ coordinated to an anionic fragment $[Ln(OSSO)_2]^-$. One of the three [OSSO]-type ligands is exclusively bonded to only one metal center (La2). The two remaining ligands are coordinated to the other lanthanum center. In each of these ligands, one of the phenolate oxygen atoms is bridging both metal atoms. Taking into account the interactions to both oxygen and to sulfur, 8-fold coordination and thus a double-capped octahedral geometry for each lanthanum center in **6d** results. The molecule displays C_1-symmetry in the solid state, but the bis(phenolato) moiety at La2 nearly possesses C_s-symmetry relative to a mirror plane defined by La1−O2−La2−O4. The other two bis(phenolato) ligands are nearly C_2-symmetric with regard to each other, with the symmetry axis along the La1−La2 axis. The La−S bond lengths in **6d** show a broad variation. Some of them are significantly larger than those in a reported lanthanum complex with a thiacrown ether ligand (3.0891(4)−3.1263(4) Å),[22] indicating weak coordination interactions to the sulfur atoms. This explains the formation of a symmetric structure of **6d** in a mixture of C_6D_6/THF-d_8 (vide supra). The addition of THF apparently results in the dissociation of sulfur atoms from the lanthanum centers and thereby facilitates the configurational change of the bis(phenolato) ligand skeleton to form a symmetric structure. The terminal La−O bond lengths in **6d** (2.242(7)–2.273(5) Å) are comparable to values reported for terminal La−O bonds (2.229(3)–2.315(3) Å).[11a] The La1−La2 distance of 4.0705(8) Å also falls within the normal range of 3.997–4.096 Å.

Ring-Opening Polymerization of *rac*-Lactide. As can been seen from the data compiled in Table 4, the yttrium complexes **1b**−**9b** and the lutetium complexes **1c**−**3c** were highly active in the polymerization of *rac*-LA in THF at ambient temperature. High conversion of monomer to PLA was achieved within 1 h. Similar to our previous results,[11d,15] complexes with a C_2-bridged ligand are generally more active than those with ligand systems featuring longer links under the same conditions. All of the yttrium and lutetium complexes are significantly more active than the corresponding scandium complexes.[11d,15a,b]

The resulting PLAs have high number-average molecular weights that slightly deviate from the theoretical values. Significant deviations are observed especially for the lutetium complexes (entries 26, 29). We explain this by partial deactivation of the rare-earth metal complexes during the polymerization process. The molecular weight distributions of the PLAs obtained by these yttrium and lutetium complexes are narrower compared to those obtained by the scandium analogues but still broader than that expected for a living polymerization. A relatively slow initiation step by the less electrophilic silylamide ligand during the polymerization procedure may account for this.[15b,23]

(22) Karmazin, L.; Mazzanti, M.; Pécaut, J. *Chem. Commun.* **2002**, 654–655.

(23) (a) Chisholm, M. H.; Delbridge, E. E. *New J. Chem.* **2003**, *27*, 1177–1183. (b) Chisholm, M. H.; Delbridge, E. E.; Galucci, J. C. *New J. Chem.* **2004**, *6*, 145–152. (c) Chisholm, M. H.; Galucci, J.; Krempner, C.; Wiggenhorn, C. *Dalton Trans.* **2006**, 846–851.

Table 4. Ring-Opening Polymerization of Lactides at Room Temperature by Rare-Earth Metal Complexes $[Ln(OSSO)\{N(SiHMe_2)_2\}(THF)_n]$ [a]

entry	init.	monomer	$[LA]_0/[Ln]_0$	*t* (h)	conv.[h] (%)	$M_{n,cald}$[i] ($\times10^4$)	$M_{n,exp}$[k] ($\times10^4$)	M_w/M_n[k]	P_r[l]
1	**1b**	*rac*-LA	300	1	94	4.06	3.14	1.66	0.68
2	**1b**	*rac*-LA	1500[b]	2	78	16.9	14.8	1.90	0.68
3	**2b**	L-LA	300	0.15	94	4.06	6.90	1.58	-
4	**2b**	L-LA	750	0.5	95	10.3	14.0	1.59	-
5	**2b**	*rac*-LA	300	0.15	95	4.11	5.09	1.62	0.71
6	**2b**	*rac*-LA	750	0.5	98	10.6	10.0	1.99	0.71
7	**2b**	*rac*-LA	750[c]	2	81	8.75	12.4	1.59	0.72
8	**3b**	L-LA	300	0.17	80	3.46	5.20	1.74	-
9	**3b**	L- LA	3000[b]	6	64	27.7	26.5	1.77	-
10	**3b**	*rac*-LA	300	0.17	90	3.89	3.71	1.60	0.72
11	**3b**	*rac*-LA	3000[b]	6	79	34.2	22.6	1.95	0.70
12	**5b**	L-LA	300	24	97	4.19	2.93	1.28	-
13	**5b**	*rac*-LA	300	2	90	3.89	3.53	1.52	0.84
14	**5b**	*rac*-LA	300[d,e]	0.83	98	2.12[j]	1.90	1.27	0.51
15	**5b**	*rac*-LA	300[d,f]	0.3	97	1.40[j]	1.43	1.12	0.51
16	**6b**	L-LA	300	2	80	3.46	3.34	1.28	-
17	**6b**	*rac*-LA	300	0.5	81	3.50	4.43	1.59	0.85
18	**6b**	*rac*-LA	3000[g]	4	89	38.5	21.2	1.77	0.84
19	**7b**	L-LA	300	2	93	4.02	3.65	1.31	-
20	**7b**	*rac*-LA	300	0.5	85	3.68	5.01	1.33	0.86
21	**7b**	*rac*-LA	300	1	93	4.02	4.54	1.45	0.86
22	**7b**	*rac*-LA	3000[g]	4	91	39.3	20.4	1.74	0.85
23	**9b**	L-LA	300	2.5	66	2.85	3.29	1.19	-
24	**9b**	*rac*-LA	300	0.75	89	3.85	3.07	1.74	0.88
25	**9b**	*rac*-LA	3000[b]	6	92	39.8	18.3	2.07	0.88
26	**1c**	*rac*-LA	300	0.2	92	3.98	9.05	1.89	0.64
27	**3c**	L-LA	300	0.1	63	2.72	10.8	1.43	-
28	**3c**	*rac*-LA	300	0.1	78	3.37	8.47	1.64	0.67
29	**3c**	*rac*-LA	300	0.5	91	3.93	8.70	1.54	0.67
30	**3c**	*rac*-LA	3000[b]	3	93	40.2	51.4	1.57	0.66
31	**6c**	L-LA	300	2	81	3.50	52.4	1.43	-
32	**6c**	*rac*-LA	300	2	94	4.06	4.72	1.62	0.82
33	**6c**	*rac*-LA	750	4	98	10.6	8.93	1.79	0.81

[a] $[Ln]_0 = 2.9$ mmol/L, THF 1 mL. [b] $[Ln]_0 = 1.45$ mmol/L, THF 1 mL. [c] $[Ln]_0 = 1.45$ mmol/L, THF 2 mL. [d] Toluene, 1 mL. [e] 2-Propanol was added, $[{}^iPrOH]_0/[Ln]_0 = 2$. [f] 2-Propanol was added, $[{}^iPrOH]_0/[Ln]_0 = 3$. [g] $[Ln]_0 = 0.29$ mmol/L, THF 1 mL. [h] Monomer conversion determined by ^1H NMR spectroscopy. [i] $M_{n,calcd} = ([LA]_0/[Ln]_0) \times 144.13 \times$ conv %. [j] $M_{n,calcd} = (300 \times 144.13 \times \text{conv } \%)/n, n = [{}^iPrOH]_0/[Ln]_0$. [k] Determined by GPC and corrected using the Mark–Houwink factor of 0.58. [l] Probability of forming a new *r*-dyad, determined by homonuclear decoupled ^1H NMR spectroscopy.

The microstructure analysis[10b,24] of PLAs formed from *rac*-LA with yttrium complexes **1b**−**9b** and lutetium complexes **1c**−**3c** revealed that the ligand sphere and the nature of the metal center exert a significant influence on the tacticity of the growing polymer chain. All the complexes show substantial heterotactic selectivity with a maximum P_r of 0.88 observed for the yttrium complex **9b**. Similar to the observations previously made for scandium complexes,[11d] the heterotactic selectivity of yttrium complexes **1b–9b** is apparently enhanced when the steric demand of the bis(phenolato) ligand is increased either by the length of the bridge or by bulky *ortho*-substituents in the phenoxy unit. The influence of the bridging moiety is most significant (Table 5). The most notable surge in heterotacticity is observed with the extension of the bridging unit from C_2 to C_3, where the P_r value increases from 0.68 for complex **1b** to 0.84 for complex **5b**. Exchanging the *ortho*-substituent *tert*-butyl against cumyl results only in slight improvement to 0.71 for complex **2b**. A further increase in the length of the bridging unit to a C_4 bridge in the bis(phenolato) ligands of complexes **6b**−**9b** did not bring any further improvement in heteroselectivity. The chirality of the ligand skeleton in complexes

Table 5. Summary of Heterotactic Selectivity during ROP of *rac*-Lactide by Rare-Earth Metal Complexes $[Ln(OSSO)\{N(SiHMe_2)_2\}(THF)_n]$[a]

	bridge	R^1	R^2	Ligand	P_r		
					Sc[11d]	Y	Lu
C_2	-$(CH_2)_2$-	^{t}Bu	Me	**1**	0.78	0.68	0.64
	-$(CH_2)_2$-	cumyl	cumyl	**2**	0.80	0.71	–
	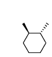	^{t}Bu	Me	**3**	0.82	0.72	0.67
C_3	-$(CH_2)_3$-	^{t}Bu	Me	**4**	0.95	–	–
	-$(CH_2)_3$-	^{t}Bu	^{t}Bu	**5**	–	0.84	–
C_4	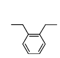	^{t}Bu	Me	**6**	0.94	0.85	0.82
	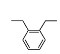	cumyl	cumyl	**7**	–	0.86	–
	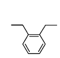	1-ada	Me	**8**	0.93	–	–
	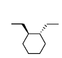	^{t}Bu	Me	**9**	0.94	0.88	–

[a] $[LA]_0/[Ln]_0 = 300$, $[Ln]_0 = 2.9$ mmol/L, THF, refer entries in Table 4 for detail. [b] Probability of forming a new *r*-dyad, determined by homonuclear decoupled ^1H NMR spectroscopy.

(24) Polylactide characterization: (a) Chisholm, M. H.; Iyer, S. S.; Matison, M. E.; McCollum, D. G.; Pagel, M. *Chem. Commun.* **1997**, 1999–2000. (b) Thakur, K. A. M.; Kean, R. T.; Hall, E. S. *Anal. Chem.* **1997**, *69*, 4303–4309. (c) Thakur, K. A. M.; Kean, R. T.; Zell, M. T.; Padden, B. E.; Munson, E. J. *Chem. Commun.* **1998**, 1913–1914.

Scheme 4

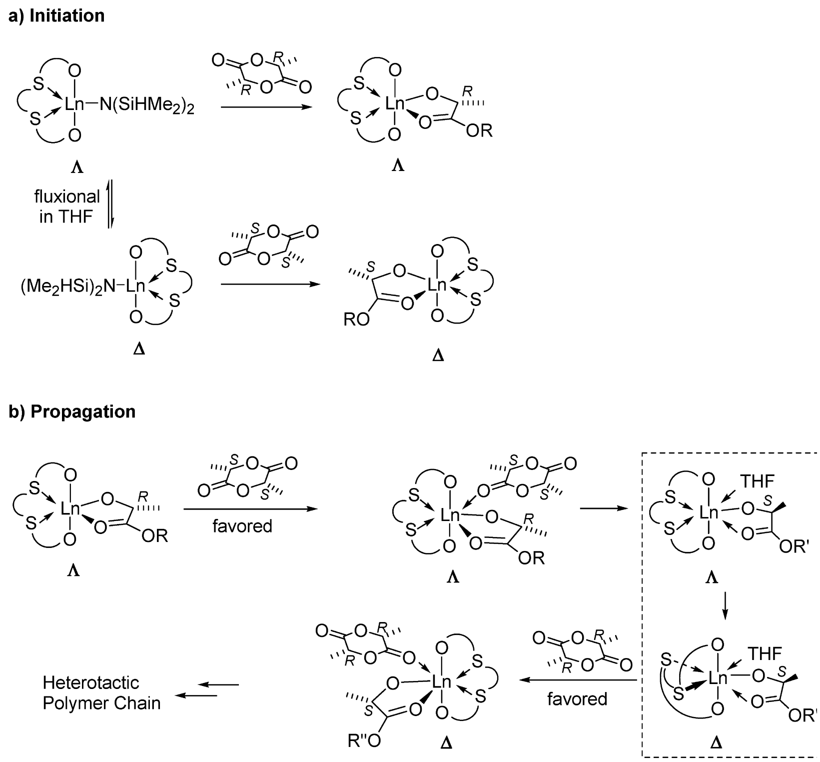

3b, **3c**, and **9b** has no influence on the tacticity and thereby suggests the absence of a normal enantiomorphic site control during ROP of *rac*-LA by these rare-earth metal complexes.

In our previous work, a model complex which is believed to mimic the catalytically active species or intermediate of the stereoselective ROP of *rac*-lactide was obtained from the reaction of [Sc(xytbm){(NSiHMe$_2$)$_2$}(THF)] and (*R*)-(+)-butyl lactate.[11d] On the basis of its structure, a dynamic monomer recognition process was proposed to explain the origin of the high heteroselectivity of bis(phenolato) scandium complexes for the ROP of *rac*-lactide.[11d] This mechanism is also thought to be operative for yttrium and lutetium complexes supported by the same series of bis(phenolato) ligands. As illustrated in Scheme 4, after the insertion of either enantiomer of *rac*-lactide in the initiation step, the bulky chiral environment around the metal center generated by the ligand framework will allow one of the enantiomers (L-lactide in Scheme 4) to approach and coordinate to the metal center. After ring-opening of the coordinated monomer, the steric repulsion between the α-methyl group of the ring-opened monomer and the *ortho*-substitutent of the ligand will induce a transformation between Λ and Δ configuration of the ligand. The Δ configuration will preferentially attack D-lactide, eventually leading to a heterotactic polymer chain.

To achieve this dynamic monomer recognition, fluxionality of the ligand framework is a prerequisite. For complexes bearing a C$_2$-bridged bis(phenolato) ligand, the two protons of the SCH$_2$ unit are chemically inequivalent as shown by a typical AB spin pattern in the ^{1}H NMR spectra (THF-d_8, 25 °C), which indicates the lack of fluxionality of a C$_2$ bridge. For complexes bearing C$_3$-bridged bis(phenolato) ligands such as the yttrium complex **5b**, all four protons of two SCH$_2$ units are always chemically equivalent and are recorded as distinct triplets in the ^{1}H NMR spectra (C$_6$D$_6$ or THF-d_8). This implies that the C$_3$ bridge allows a free configurational transformation of the ligand framework. In agreement with this result, a surge of heterotactic selectivity in ROP of *rac*-lactide was observed for complex **5b** bearing a C$_3$-bridged ligand as compared to complexes **1b**−**3b** containing the C$_2$-bridged ligands. For complex **2b**, the cumyl group in the *ortho*-position of the phenoxy ligand increases the congestion at the metal center, but the rigid C$_2$ bridge restricts a flexible configuration transformation, resulting only in slight improvement of the heteroselectivity. Only slight increase in the heteroselectivity during ROP of *rac*-lactide was observed for complexes **6b**−**9b**, likely caused by the increase of the steric bulkiness of the ligands. It is also possible that the C$_4$-bridged units involved in these ligands are somewhat rigid compared to aliphatic alkanediyl-linked systems. The influence of the C$_3$ bridge compared to the C$_2$ bridge was also observed for aluminum complexes with tetradentate Schiff base ligands,[5i] where the high isotactic selectivity for ROP of *rac*-lactide was obtained for complexes with the C$_3$-bridged ligand. However, further increasing the bridge length in this aluminum system led to a decrease of isoselectivity. Obviously, different stereocontrol processes may be operative here.[5q]

As can be seen from Table 5, the heteroselectivity during ROP of *rac*-LA is increased for metal complexes of a given ligand (**1**, **3**, and **6**) in the order Sc (**a**) > Y (**b**) > Lu (**c**). Compared to yttrium and lutetium, scandium is significantly smaller. Therefore, a given ligand will form a more crowded coordination environment at scandium in comparison to the situation at yttrium and lutetium, resulting in higher heteroselectivity. As the radius of yttrium is somewhat larger than that of lutetium, the heteroselectivity could be expected to be lower. However, the lutetium complexes, generally more active than the yttrium analogues, show decreased heteroselectivity.

Yttrium complexes **6b−9b** show higher heterotactic selectivity and are highly efficient for the ROP of *rac*-lactide. Remarkably high conversions up to 91% for 3000 equiv of monomer to PLAs can be achieved within hours using relatively low initiator concentrations (entries 18, 22, and 25). The tacticities of the obtained polymers are determined by the initiator, regardless of their high molecular weights up to 887 000 g mol^{-1}. Compared to the high efficiency toward *rac*-lactide, complexes **6b−9b** polymerize L-lactide rather slowly, reflecting the high selectivity for alternating enchainment of L-lactide and D-lactide (entries 16 vs 17, 19 vs 20, and 23 vs 24). As reported previously,[11d] the use of THF as solvent is crucial for the high heteroselectivity and activity by these complexes during the ROP of *rac*-LA. Polymerization runs in toluene only afforded traces of polymers after several days. The addition of excess alcohol to the initiator/*rac*-LA mixture in toluene accelerates the polymerization to give atactic PLAs in a controlled manner (entries 14 and 15). The crucial role of THF for high heterotactic selectivity has also been reported for some well-defined zinc, calcium, and yttrium initiator systems.[9a,10b,11b] More recently, a related alkoxyamine bis(phenolato) yttrium complex has been reported to show heteroselective and immortal behavior in the presence of 2-propanol.[11f]

Conclusions

Utilizing the well-established amine elimination method, several monomeric yttrium and lutetium complexes supported by sulfur-bridged bis(phenolato) ligands of [OSSO]-type were synthesized and structurally characterized. This series of yttrium and lutetium complexes efficiently initiated the ring-opening polymerization of *rac*-lactide in THF. High heterotacticity was observed for the resultant poly(lactide) chains. Increase in heteroselectivity during the ROP of *rac*-lactide by these complexes was observed with increasing steric bulk of the bis(phenolato) ligands. The influence of the bridging moiety is most significant. On the basis of the structure of a model complex of scandium, "a dynamic enantiomorphic site control"[11d,12g] resulting from the configurational interconversion of the active site during the polymerization was suggested to be responsible for the observed high heteroselectivity. Thus a C_3 or C_4 bridge allows sufficient fluxionality of the ligand framework to enable the interconversion between Λ to Δ configurations, responsible for enantiomer recognition.

Experimental Section

General Considerations. All operations were performed under an inert atmosphere of argon using standard Schlenk-line or glovebox techniques. Toluene, *n*-hexane, and THF were distilled under argon from sodium/benzophenone ketyl prior to use. *n*-Pentane was purified by distillation from sodium/triglyme benzophenone ketyl. Dichloromethane was distilled from calcium hydride. Anhydrous lanthanide trichlorides (Aldrich or Strem products) were used as received. Benzene-d_6, chloroform-*d*, and other reagents were carefully dried and stored in a glovebox. [Ln{N(SiHMe$_2$)$_2$}$_3$(THF)$_x$] (Ln = Sc, Y, Lu; x = 1, 2) were synthesized according to the literature methods.[21,25] 4,6-Di(2-phenyl-2-propyl)-2-thiophenol was synthesized according to a modification of the method reported in the literature.[26] 1,4-Dithiabutanediyl-2,2′-bis{4,6-di(2-phenyl-2-propyl)phenol}, etccpH$_2$ (**2**),[26] *ortho*-xylylenedithiobis(6-*tert*-butyl-4-methylphenol), xytbmpH$_2$ (**6**),[27] *ortho*-xylylenedithiobis(6-adamantyl-4-methylphenol), xytampH$_2$ (**8**),[11d] and *rac*-(3,4-*trans*-butanediyl-1,6-dithiahexanediyl)-2,2′-bis(6-*tert*-butyl-4-methylphenol), cmtbmpH$_2$ (*rac*-**9**),[11d] were prepared according to reported methods. L-Lactide and *rac*-lactide (Aldrich) were recrystallized from dry toluene and sublimed twice under vacuum at 50 °C. 2-Propanol was dried over calcium hydride prior to distillation. All other chemicals were commercially available and used after appropriate purification. Glassware and vials used in the polymerization were dried in an oven at 120 °C overnight and exposed to vacuum−argon cycle three times.

NMR spectra were recorded on Bruker DRX 400, Varian 200 and 500 spectrometers at 25 °C (^{1}H: 200, 400, 500 MHz; ^{13}C: 50, 100, 125 MHz) unless otherwise stated. Chemical shifts for ^{1}H and ^{13}C NMR spectra were referenced internally using the residual solvent resonances and reported relative to tetramethylsilane. NMR assignments were confirmed by Apt, ^{1}H−^{1}H (COSY), and ^{1}H−^{13}C (HMQC) when necessary. Elemental analyses were performed by the Microanalytical Laboratory of University of Mainz, Germany. Spectroscopic analysis of polymers was performed in $CDCl_3$. Molecular weights and polydispersities of polymer samples were determined by size exclusion chromatography (GPC) in THF at 35 °C, at a flow rate of 1 mL/min utilizing an Agilent 1100 Series HPLC, G1310A isocratic pump, an Agilent 1100 Series refractive index detector and 8 × 600 mm, 8 × 300 mm, 8 × 50 mm PSS SDV linear M columns. Calibration standards were commercially available narrowly distributed linear polystyrene samples that cover a broad range of molar masses ($10^3 < M_n < 2 \times 10^6$ g mol^{-1}).

***rac*-(2,3-*trans*-butanediyl-1,4-dithiabutanediyl)-2,2′-bis(6-*tert*-butyl-4-methylphenol), cytbmpH$_2$ (*rac*-3)**[28]. Solid sodium hydroxide (4.908 g, 0.123 mmol) was added to a solution of 4-methyl-6-*tert*-butyl-2-thiophenol (24.051 g, 0.123 mmol) in methanol (100 mL). The mixture was exposed to ultrasound until sodium hydroxide dissolved. Cyclohexene oxide (12.043 g, 0.123 mmol) was added dropwise via syringe to the yellow solution and the mixture was heated to reflux for 2 h. All volatiles were removed in vacuum from the reaction mixture. The solid residue was extracted with diethyl ether and washed with water (3 × 100 mL). The pale yellow organic phase was separated, dried over anhydrous sodium sulfate, and evaporated to dryness to give 4-methyl-6-*tert*-butyl-2-(*trans*-2-hydroxycyclohexyl)thiophenol as a pale yellow viscous liquid (35.134 g, 97%) which was pure by ^{1}H NMR spectroscopy. ^{1}H NMR ($CDCl_3$, 200 MHz): δ 7.15 (d, 1H, $^4J_{HH}$ = 1.6 Hz), 7.09

(25) (a) Herrmann, W. A.; Anwander, R.; Munck, F. C.; Scherer, W.; Dufaud, V.; Huber, N. W.; Artus, G. R. J. *Z. Naturforsch. B.* **1994**, *49*, 1789–1797. (b) Herrmann, W. A.; Munck, F. C.; Artus, G. R. J.; Runte, O.; Anwander, R. *Organometallics* **1997**, *16*, 682–688.

(26) (a) Capacchione, C.; Proto, A.; Ebeling, H.; Mülhaupt, R.; Möller, K.; Spaniol, T. P.; Okuda, J. *J. Am. Chem. Soc.* **2003**, *125*, 4964–4965. (b) Capacchione, C.; Manivannan, R.; Barone, M.; Beckerle, K.; Centore, R.; Oliva, L.; Proto, A.; Tuzi, A.; Spaniol, T. P.; Okuda, J. *Organometallics* **2005**, *24*, 2971–2982.

(27) Ma, H.; Melillo, G.; Oliva, L.; Spaniol, T. P.; Englert, U.; Okuda, J. *Dalton Trans.* **2005**, 721–727.

(28) Beckerle, K.; Manivannan, R.; Lian, B.; Meppelder, G.-J. M.; Raabe, G.; Spaniol, T. P.; Ebeling, H.; Pelascini, E.; Mülhaupt, R.; Okuda, J. *Angew. Chem., Int. Ed.* **2007**, *46*, 4790–4793.

(d, 1H, $^4J_{HH}$ = 1.6 Hz), 3.35 (m, 1H, cyclohexyl-*H*), 2.56 (m, 1H, SC*H*), 2.26 (s, 3H, CH_3), 2.08 (m, 2H, cyclohexyl-*H*), 1.68 (m, 2H, cyclohexyl-*H*), 1.40 (s, 9H, C(CH_3)), 1.24 (m, 4H, cyclohexyl-*H*).

Thionyl chloride (5.542 g, 46.01 mmol) was added dropwise via syringe to the solution of 4-methyl-6-*tert*-butyl-2-(*trans*-2-hydroxycyclohexyl)thiophenol (11.29 g, 38.34 mmol) in dichloromethane (100 mL) at −30 °C. The reaction mixture was warmed slowly to room temperature and heated to reflux for 5 h. After cooling, the reaction mixture was concentrated to dry to remove the excess $SOCl_2$. The obtained residue was treated with water and diethyl ether for 10 min. After extraction with diethyl ether and sequential washing with water, aqueous sodium bicarbonate solution and water, the organic layer was dried over anhydrous sodium sulfate. After workup and removal of the solvent under vacuum, 4-methyl-6-*tert*-butyl-2-(*trans*-2-chlorocyclohexyl)thiophenol (11.85 g, 98%) was obtained as a viscous, pale orange liquid, which was pure by ^{1}H NMR spectroscopy. ^{1}H NMR (CDCl$_3$, 200 MHz): δ 7.23 (s, 1H, O*H*), 7.17 (d, 1H, $^4J_{HH}$ = 2.2 Hz), 7.10 (d, 1H, $^4J_{HH}$ = 2.2 Hz), 3.84 (td, 1H, $^3J_{a,a}$ = 9.0 Hz, $^3J_{a,e}$ = 4.0 Hz, ClC*H*), 2.88 (td, 1H, $^3J_{a,a}$ = 9.0 Hz, $^3J_{a,e}$ = 4.0 Hz, SC*H*), 2.44–2.28 (m, 1H, cyclohexyl-*H*), 2.26 (s, 3H, CH_3), 2.23–2.08 (m, 1H, cyclohexyl-*H*), 1.85–1.59 (m, 4H, cyclohexyl-*H*), 1.40 (s, 9H, C(CH_3)), 1.39 (m, 2H, overlapped, cyclohexyl-*H*).

Sodium hydroxide (1.037 g, 25.93 mmol) was added to the solution of 4-methyl-6-*tert*-butyl-2-thiophenol (5.082 g, 25.93 mmol) in methanol (20 mL). The mixture was exposed to ultrasound until the sodium hydroxide dissolved completely to give a yellow solution. A solution of 4-methyl-6-*tert*-butyl-2-(2-chlorocyclohexyl)-thiophenol (8.113 g, 25.93 mmol) in the mixture of methanol and dichloromethane (50 mL/40 mL) was added dropwise to the above yellow solution. The reaction mixture was heated to reflux for 2 h, white solids precipitated gradually. After cooling, the white solids were collected by suction, washed with a small amount of methanol and dried under vacuum. The solids were dissolved in dichloromethane and filtrated. After removal of solvent, the solid was recrystallized with hexane to afford needle-like, colorless crystals (13.2 g, 83%). ^{1}H NMR (CDCl$_3$, 200 MHz): δ 7.40 (s, 2H, O*H*), 7.18 (d, 2H, $^4J_{HH}$ = 2.0 Hz), 7.10 (d, 2H, $^4J_{HH}$ = 2.0 Hz), 2.75 (m, 2H, SC*H*), 2.25 (s, 6H, CH_3), 2.04 (m, 2H, cyclohexyl-*H*), 1.65 (m, 2H, cyclohexyl-*H*), 1.41 (s, 18H, C(CH_3)), 1.40 (m, 2H, overlapped, cyclohexyl-*H*), 1.21 (m, 2H, cyclohexyl-*H*). ^{13}C{^{1}H} NMR (CDCl$_3$, 50 MHz): δ 154.0 (Ar-*C*1), 135.6 (Ar-*C*6), 134.7 (Ar-*C*4), 129.7 (Ar-*C*3), 128.3 (Ar-*C*5), 116.4 (Ar-*C*2), 52.8 (S*C*H), 34.9 (6-*C*(CH$_3$)), 33.4 (cyclohexyl-*C*), 29.5 (6-C(*C*H$_3$)), 25.4 (cyclohexyl-*C*), 20.7 (4-*C*H$_3$). Anal. Calcd for $C_{28}H_{40}O_2S_2$: C, 71.14; H, 8.53; S, 13.57. Found: C, 71.02; H, 8.56; S, 13.6.

***ortho*-Xylylenedithio-bis{4,6-di(2-phenyl-2-propyl)phenol}, xytccpH$_2$ (7).** Under argon, to the solution of 4,6-di(2-phenyl-2-propyl)-2-thiophenol (9.060 g, 24.9 mmol) in a mixture of methanol and toluene (25 mL/5 mL) was added slowly solid sodium hydroxide (0.997 g, 24.9 mmol) at 50 °C. The obtained yellow solution was further treated dropwise with a solution of 1,2-bis(bromomethyl)benzene (3.289 g, 12.46 mmol) in toluene (20 mL). The reaction solution was stirred overnight at 60 °C to give a mixture of white solids, a colorless solution, and a viscous orange yellow oil. All the volatiles were removed under vacuum. The residue was dissolved with *n*-pentane (80 mL) and filtered. The filtrate was kept at 0 °C for 4 h; colorless prismatic crystals were obtained (5.95 g, 57%). ^{1}H NMR (CDCl$_3$, 200 MHz): δ 7.32–7.09 (m, 22H, Ar-*H*), 7.00 (m, 2H, Ar-*H*), 6.83 (d, 2H, $^4J_{HH}$ = 2.2 Hz, 3-*H*), 6.66 (m, 2H, Ar-*H*), 6.41 (s, 2H, O*H*), 3.45 (s, 4H, SCH_2), 1.54 (s, 24H, CH_3). ^{13}C{^{1}H} NMR (C$_6$D$_6$, 50 MHz): δ 153.0 (*C*1), 150.5, 150.2, 141.4, 135.4 (Ar-*C*6), 134.3, 132.5, 130.5 (*C*3), 127.92, 127.87 (*C*4), 127.78, 127.3, 126.5, 125.52, 125.48, 125.2, 117.1 (*C*2), 42.4 (S*C*H$_2$), 42.3 (*C*(CH$_3$)$_2$), 30.8 (*C*H$_3$), 29.3 (*C*H$_3$). Anal. Calcd for $C_{56}H_{58}O_2S_2$: C, 81.31; H, 7.07; S, 7.75. Found: C, 81.22; H, 7.12; S, 7.54.

[Y(etccp){N(SiHMe$_2$)$_2$}(THF)] (2b). A solution of 1,4-dithiabutanediyl-2,2′-bis{4,6-di(2-phenyl-2-propyl)phenol} (etccpH$_2$) (0.376 g, 0.500 mmol) in toluene (5 mL) was added slowly to a solution of [Y{N(SiHMe$_2$)$_2$}$_3$(THF)$_2$] (0.315 g, 0.500 mmol) in toluene (10 mL) at room temperature. The yellow solution was stirred for 8 days at 50 °C. The obtained slightly pale yellow solution was concentrated to dryness to afford a foam-like solid, which was further dried under high vacuum for several hours. The solid obtained was then dissolved with 10 mL of *n*-pentane and filtered. The clear filtrate was concentrated to dryness to give a white powder in quantitative yield. ^{1}H NMR (C$_6$D$_6$, 500 MHz): δ 7.46 (d, 2H, $^4J_{HH}$ = 2.0 Hz), 7.28 (br d, 4H), 7.26 (dd, 4H, $^3J_{HH}$ = 8.5 Hz, $^4J_{HH}$ = 1.5 Hz), 7.21 (d, 2H, $^4J_{HH}$ = 2.5 Hz), 7.16–7.10 (m, 8H), 7.03 (tt, 2H, $^3J_{HH}$ = 7.5 Hz, $^4J_{HH}$ = 1.5 Hz), 6.95 (tt, 2H, $^3J_{HH}$ = 7.5 Hz, $^4J_{HH}$= 1.5 Hz), 4.93 (septet, 2H, $^3J_{HH}$ = 3.0 Hz, Si*H*), 2.92 (m, 4H, THF), 2.36 (br d, 4H, SCH_2), 1.80 (br s, 12H, CH_3), 1.62 (s, 12H, CH_3), 0.98 (m, 4H, THF), 0.33 (d, 12H, $^3J_{HH}$ = 3.0 Hz, Si(CH_3)$_2$). ^{13}C{^{1}H} NMR (C$_6$D$_6$, 125 MHz): δ 166 (*C*1), 152.1 (Ar-*C*), 151.6 (Ar-*C*), 138.2 (*C*6), 137.1 (*C*4), 130.5 (*C*3), 128.5(*C*5), 127.0 (Ar-*C*), 126.3 (Ar-*C*), 125.8 (Ar-*C*), 124.8 (Ar-*C*), 118.1 (*C*2), 70.3 (THF), 43.0 (S *C*H$_2$), 42.7 (*C*(CH$_3$)$_2$), 31.3 (*C*H$_3$), 25.1 (THF), 3.7 (Si(CH$_3$)$_2$). Anal. Calcd for $C_{58}H_{74}NO_3S_2Si_2Y\cdot0.1(C_7H_8)$: C, 67.04; H, 7.17; N, 1.33; S, 6.10. Found: C, 67.56; H, 7.32; N, 1.88; S, 6.35.

[Y(cytbmp){N(SiHMe$_2$)$_2$}(THF)] (3b). Solid cytbmpH$_2$ (0.236 g, 0.500 mmol) was added slowly to a solution of [Y{N(SiHMe$_2$)$_2$}$_3$(THF)$_2$] (0.315 g, 0.500 mmol) in *n*-pentane (15 mL) at room temperature. The colorless solution was stirred for 5 days, and all the volatiles were removed in vacuo to afford a white solid, which was further dried under high vacuum for several hours. The solid obtained was then dissolved with *n*-hexane. After filtration, the filtrate was concentrated to about 3 mL and kept at −40 °C to give colorless crystals (300 mg, 79%, two crops). ^{1}H NMR (C$_6$D$_6$, 500 MHz): δ 7.28 (d, 2H, $^4J_{HH}$ = 2.4 Hz, 5-*H*), 7.17 (d, 2H, $^4J_{HH}$ = 2.4 Hz, 3-*H*), 5.22 (septet, 2H, Si*H*, $^3J_{HH}$ = 3.0 Hz), 3.94 (br s, 4H, THF), 2.68 (br s, 2H, SC*H*), 2.19 (s, 6H, CH_3), 1.89 (br s, 2H, cyclohexyl-*H*), 1.72 (s, 18H, C(CH_3)$_3$), 1.65 (br s, 2H, cyclohexyl-*H*), 1.17 (m, 4H, THF), 1.06 (br s, 2H, cyclohexyl-*H*), 0.43 (d, 6H, $^3J_{HH}$ = 3.0 Hz, Si(CH_3)$_2$), 0.41 (d, 6H, $^3J_{HH}$ = 3.0 Hz, Si(CH_3)$_2$), 0.39 (br s, 2H, cyclohexyl-*H*, overlapped). ^{13}C{^{1}H} NMR (C$_6$D$_6$, 125 MHz): δ 167.4 (*C*1), 138.5 (*C*6), 135.5 (*C*3), 130.8 (*C*5), 123.7 (*C*4), 115.7 (*C*2), 71.2 (THF), 53.2 (S *C*H$_2$), 35.6 (6-*C*(CH$_3$)$_3$), 34.5 (cyclohexyl-*C*), 29.9 (6-C(*C*H$_3$)$_3$), 25.5 (cyclohexyl-*C*), 25.1 (THF), 20.9 (4-*C*H$_3$), 3.7 (Si(*C*H$_3$)$_2$). Anal. Calcd for $C_{36}H_{60}NO_3S_2Si_2Y$: C, 56.59; H, 7.91; N, 1.83; S, 8.39. Found: C, 56.92; H, 8.41; N, 2.16; S, 8.42.

[Lu(cytbmp){N(SiHMe$_2$)$_2$}(THF)] (3c). Solid cytbmpH$_2$ (0.236 g, 0.500 mmol) was added slowly to a solution of [Lu{N(SiHMe$_2$)$_2$}$_3$(THF)$_2$] (0.357 g, 0.500 mmol) in *n*-pentane (15 mL) at room temperature. The colorless solution was stirred for 5 days. After filtration to remove trace amount of solid, all the volatiles were removed in vacuo to afford a solid foam, which was dried under high vacuum for several hours. The solid obtained was then dissolved in *n*-hexane (4 mL) and kept at −40 °C to give colorless crystals (260 mg, 61%, two crops). ^{1}H NMR (C$_6$D$_6$, 500 MHz): δ 7.29 (d, 2H, $^4J_{HH}$ = 2.1 Hz, 5-*H*), 7.15 (2H, 3-*H*, overlapped by solvent signal), 5.2 (septet, 2H, $^3J_{HH}$ = 3.0 Hz, Si*H*), 3.95 (br s, 4H, THF), 2.64 (br s, 2H, SC*H*), 2.19 (s, 6H, CH_3), 1.85 (br d, 2H, cyclohexyl-*H*), 1.73 (s, 18H, C(CH_3)$_3$), 1.63 (br d, 2H, cyclohexyl-*H*), 1.14 (m, 4H, THF), 1.02 (br d, 2H, cyclohexyl-*H*), 0.46 (d, 6H, $^3J_{HH}$ = 3.0 Hz, Si(CH_3)$_2$), 0.43 (d, 6H, $^3J_{HH}$ = 3.0 Hz, Si(CH_3)$_2$), 0.36 (br t, 2H, cyclohexyl-*H*, overlapped). ^{13}C{^{1}H} NMR (C_6D_6, 125 MHz): δ 168.3 (*C*1), 139.2 (*C*6), 135.5 (*C*3), 131.0 (*C*5), 123.6 (*C*4), 115.1 (*C*2), 71.6 (THF), 53.2 (S *C*H_2), 35.5 (6-*C*(CH$_3$)$_3$), 34.4 (cyclohexyl-*C*), 30.0 (6-C(*C*H$_3$)$_3$), 25.5 (cyclohexyl-*C*), 25.1 (THF), 20.9 (4-*C*H$_3$), 3.9 (Si(*C*H$_3$)$_2$), 3.8 (Si(*C*H$_3$)$_2$). Anal. Calcd for $C_{36}H_{60}NLuO_3S_2Si_2$: C, 50.86; H, 7.11; N, 1.65; S, 7.54. Found: C, 51.01; H, 7.50; N, 1.94; S, 7.52.

[Y(xytbmp){N(SiHMe$_2$)$_2$}(THF)] (6b). Solid xytbmpH$_2$ (0.247 g, 0.500 mmol) was added slowly to the solution of [Y{N(SiHMe$_2$)$_2$}$_3$(THF)$_2$] (0.315 g, 0.500 mmol) in *n*-hexane (10 mL) at room temperature. The colorless reaction mixture was stirred for 3 days. Some white solid precipitated and more *n*-hexane was added to dissolve the solid. After filtration to remove trace amounts of impurities, the clear solution was concentrated in vacuo to afford a white powder, which was dried for several hours. The powder obtained was recrystallized from *n*-hexane at −30 °C to afford colorless crystals (300 mg, 76%). ^{1}H NMR (C_6D_6, 400 MHz): δ 7.25 (d, 2H, $^4J_{HH}$ = 2.0 Hz, 5-*H*), 7.24 (d, 2H, $^4J_{HH}$ = 2.0 Hz, 3-*H*), 6.77 (m, 2H, Ar-*H*), 6.62 (m, 2H, Ar-*H*), 5.00 (septet, 2H, $^3J_{HH}$ = 3.0 Hz, Si*H*), 3.89 (m, 4H, THF), 3.63 (s, 4H, SC *H*$_2$), 2.28 (s, 6H, 4-CH_3), 1.60 (s, 18H, 6-C(CH_3)$_3$), 1.19 (m, 4H, THF), 0.30 (d, 12H, $^3J_{HH}$ = 3.0 Hz, Si(CH_3)$_2$). ^{13}C{^{1}H} NMR (C_6D_6, 100 MHz): δ 165.3 (*C*1), 138.1 (*C*6), 133.6 (Ar-*C*), 132.0 (*C*3), 130.6 (*C*5), 129.7(Ar-*C*), 127.9 (Ar-*C*), 124.8 (*C*4), 120.9 (*C*2), 70.6 (THF), 40.3 (S*C*H$_2$), 35.5 (6-*C*(CH$_3$)$_3$), 30.0 (6-C(*C*H$_3$)$_3$), 25.1 (THF), 20.9 (4-*C*H$_3$), 3.3 (Si(*C*H$_3$)$_2$). Anal. Calcd for $C_{38}H_{58}NO_3S_2Si_2Y$: C, 58.06; H, 7.44; N, 1.78; S, 8.16. Found: C, 57.85; H, 7.56; N, 1.96; S, 8.25.

[Lu(xytbmp){N(SiHMe$_2$)$_2$}(THF)] (6c). Solid xytbmpH$_2$ (0.247 g, 0.500 mmol) was added slowly to the solution of [Lu{N(SiHMe$_2$)$_2$}$_3$(THF)$_2$] (0.357 g, 0.500 mmol) in *n*-hexane (15 mL) at room temperature. The colorless reaction mixture was stirred for 5 days. White solids precipitated, and more *n*-hexane was added to dissolve the solid. After filtration to remove trace amounts of impurities, the clear solution was concentrated in vacuo to afford a white powder, which was dried for several hours. The powder obtained was recrystallized from *n*-heptane at −30 °C to afford colorless crystals (320 mg, 74%). ^{1}H NMR (C_6D_6, 200 MHz): δ 7.27 (d, 2H, $^4J_{HH}$ = 2.0 Hz, 5-*H*), 7.26 (d, 2H, $^4J_{HH}$ = 2.0 Hz, 3-*H*), 6.77 (m, 2H, Ar-*H*), 6.62 (m, 2H, Ar-*H*), 5.00 (septet, 2H, $^3J_{HH}$ = 3.0 Hz, Si*H*), 3.92 (m, 4H, THF), 3.64 (s, 4H, SCH_2), 2.27 (s, 6H, 4-CH_3), 1.61 (s, 18H, 6-C(CH_3)$_3$), 1.14 (m, 4H, THF), 0.30 (d, 12H, $^3J_{HH}$ = 3.0 Hz, Si(CH_3)$_2$). ^{13}C{^{1}H} NMR (C_6D_6, 50 MHz): δ 166.0 (*C*1), 138.9 (*C*6), 133.2 (Ar-*C*), 132.5 (*C*3), 130.7 (*C*5), 130.0 (Ar-*C*), 127.8 (Ar-*C*), 124.6 (*C*4), 119.9 (*C*2), 71.4 (THF), 40.8 (S*C*H$_2$), 35.6 (6-*C*(CH$_3$)$_3$), 30.1 (6-C(*C*H$_3$)$_3$), 25.1 (THF), 21.0 (4-*C*H$_3$), 3.6 (Si(*C*H$_3$)$_2$). Anal. Calcd for $C_{38}H_{58}NLuO_3S_2Si_2$: C, 52.33; H, 6.70; N, 1.61; S, 7.35. Found: C, 51.89; H, 7.07; N, 1.97; S, 7.67.

[Y(xytccp){N(SiHMe$_2$)$_2$}(THF)] (7b). Solid *ortho*-xylylenedithiobis{4,6-di(2-phenyl-2-propyl)phenol} (xytccpH$_2$) (0.414 g, 0.500 mmol) was added slowly to a solution of [Y{N(SiHMe$_2$)$_2$}$_3$(THF)$_2$] (0.315 g, 0.500 mmol) in toluene (20 mL) at room temperature. The solution was stirred for 3 days at 70 °C. The obtained slightly pale yellow solution was concentrated to dryness to afford a foam-like solid, which was further dried under high vacuum for several hours. The solid obtained was then dissolved with 10 mL of *n*-pentane and filtered. The clear filtrate was concentrated to dryness to give a white powder in quantitative yield. ^{1}H NMR (C_6D_6, 200 MHz): δ 7.45 (m, 2H), 7.42–7.37 (m, 6H), 7.29–7.20 (m, 8H), 7.11–7.04 (m, 6H), 7.16–7.10 (m, 8H), 6.93 (m, 2H), 6.82 (m, 2H), 6.55 (m, 2H), 4.80 (septet, 2H, $^3J_{HH}$ = 3.0 Hz, Si*H*), 3.58 (s, 4H, SCH_2), 2.95 (m, 4H, THF), 1.74 (12H, CH_3), 1.70 (s, 12H, CH_3), 1.06 (m, 4H, THF), 0.27 (d, 12H, $^3J_{HH}$ = 3.0 Hz, Si(CH_3)$_2$). ^{13}C{^{1}H} NMR (C_6D_6, 50 MHz): δ 166 (*C*1), 151.8 (Ar-*C*), 151.6 (Ar-*C*), 138.0 (*C*6), 136.3 (*C*4), 136.2 (Ar-*C*), 133.6 (*C*3), 130.9 (*C*5), 130.2 (Ar-*C*), 127.1 (Ar-*C*), 126.7 (Ar-*C*), 125.9 (Ar-*C*), 124.9 (Ar-*C*), 121.0 (Ar-*C*), 116.5 (*C*2), 70.1 (THF), 43.3 (S*C*H$_2$), 42.8 (*C*(CH$_3$)$_2$), 40.2 (*C*(CH$_3$)$_2$), 31.4 (*C*H$_3$), 30.5 (*C*H$_3$), 25.2 (THF), 3.4 (Si(*C*H$_3$)$_2$). Anal. Calcd for $C_{64}H_{78}NO_3S_2Si_2Y$: C, 68.73; H, 7.03; N, 1.25; S, 5.73. Found: C, 68.78; H, 7.19; N, 1.62; S, 5.67.

[Y(cmtbmp){N(SiHMe$_2$)$_2$}(THF)] (9b). A solution of cmtbmpH$_2$ (0.295 g, 0.589 mmol) in *n*-pentane (5 mL) was added slowly to a solution of [Y{N(SiHMe$_2$)$_2$}$_3$(THF)$_2$] (0.371 g, 0.589 mmol) in *n*-pentane (10 mL) at room temperature. The obtained solution was stirred for 10 days at room temperature. All the volatiles were removed in vacuo to afford a foam-like solid, which was further dried under high vacuum for several hours. The solid was then recrystallized with *n*-pentane and kept at −40 °C to give colorless crystals (190 mg, 41%). ^{1}H NMR (C_6D_6, 500 MHz): δ 7.17 (d, 2H, $^4J_{HH}$ = 2.4 Hz, 5-*H*), 7.12 (2H, $^4J_{HH}$ = 2.4 Hz, 3-*H*), 5.19 (septet, 2H, $^3J_{HH}$ = 3.0 Hz, Si*H*), 4.01 (m, 4H, THF), 2.84 (d, 2H, $^2J_{HH}$ = 13.0 Hz, SCH_2), 2.72 (dd, 2H, $^2J_{HH}$ = 13.0 Hz, $^3J_{HH}$ = 5.8 Hz, SCH_2), 2.23 (s, 6H, 4-CH_3), 1.66 (s, 18H, 6-C(CH_3)$_3$), 1.66 (2H, cyclohexyl-*H*, overlapped), 1.32 (m, 4H, THF), 1.27 (br m, 4H, cyclohexyl-*H*), 0.99 (br m, 4H, cyclohexyl-*H*), 0.40 (d, 6H, $^3J_{HH}$ = 3.0 Hz, Si(CH_3)$_2$), 0.37 (d, 6H, $^3J_{HH}$ = 3.0 Hz, Si(CH_3)$_2$). ^{13}C{^{1}H} NMR (C_6D_6, 125 MHz): δ 164.04 (*C*1), 164.02 (*C*1′), 137.8 (*C*6), 130.9 (*C*3), 128.7 (*C*5), 125.1 (*C*4), 123.6 (*C*2), 71.1 (THF), 44.2 (S*C*H$_2$), 41.1 (cyclohexyl-*C*), 35.5 (6-*C*(CH$_3$)$_3$), 31.9 (cyclohexyl-*C*), 29.9 (6-C(*C*H$_3$)$_3$), 25.2 (THF), 25.0 (cyclohexyl-*C*), 21.0 (4-*C*H$_3$), 3.5 (Si(*C*H$_3$)$_2$), 3.4 (Si(*C*H$_3$)$_2$). Anal. Calcd for $C_{38}H_{64}NO_3S_2Si_2Y$: C, 57.62; H, 8.14; N, 1.77; S, 8.10. Found: C, 58.00; H, 8.26; N, 2.00; S, 8.34.

Typical Polymerization Procedure. In a glovebox, initiator from a stock solution in THF or toluene was injected sequentially to a series of 6 mL vials loaded with L-lactide or *rac*-lactide and a suitable amount of dry solvent. After specified time intervals, each vial was taken out of the glovebox; an aliquot was withdrawn and quenched quickly with *n*-pentane; the reaction mixture was quenched at the same time by adding excess amount of *n*-pentane and one drop of water. All the volatiles in the aliquots were removed, and the residue was subjected to monomer conversion determination which was monitored by integration of monomer versus polymer methine or methyl resonances in the ^{1}H NMR spectra (CDCl$_3$, 200 MHz). The precipitates collected from the bulk mixture were dried in air, dissolved with dichloromethane, and sequentially precipitated into methanol. The obtained polymer was further dried in a vacuum oven at 60 °C for 16 h for GPC analysis. Each reaction was used as one data point. In the cases where 2-propanol was used, the initiator solution in toluene was treated first with the solution of 2-propanol in the same solvent for 10 min, and then injected to the solution of L-lactide or *rac*-lactide. Otherwise the procedures were the same.

Crystal Structure Analysis. X-ray diffraction measurements were performed on a Bruker AXS diffractometer with Mo Kα radiation using ω-scans. Crystal parameters and results of the

(29) *ASTRO, SAINT and SADABS. Data Collection and Processing Software for the SMART System*; Siemens Analytical X-ray Instruments Inc.: Madison, WI, 1996.
(30) Sheldrick, G. M. *SHELXS-86: A Program for Crystal Structure Solution*; University of Göttingen: Göttingen, Germany, 1986.

structure refinements are given in Table 1. Absorption corrections were carried with the multiscan method using SADABS.[29] All structures were solved by direct methods (SHELXS-86)[30] and refined (SHELXS-97)[31] against all F^2 data. The structure of **6d** contains the cocrystallized solvent molecules toluene and pentane in the crystal lattice which are partially disordered. For each molecule of **6d**, the unit cell contains 1.5 molecules of toluene and 0.5 molecules of pentane. Disorder is also found in one of the phenolate units. All non-hydrogen atoms except those in the disordered groups and also in solvent molecules were refined with anisotropic displacement parameters. Hydrogen atoms were included into calculated positions, and only the hydrogen atoms in **6b** that are bound to Si1 and Si2 were located in a difference Fourier map and are refined in their position. For the graphical representation, the program ORTEP was used as implied in the program system WinGX.[32] Crystallographic data (excluding structure factors) have been deposited with the Cambridge Crystallographic Data Centre as supplementary publication nos. CCDC 666471 (**6b**) and 666472 (**6d**). Copies of the data can be obtained free of charge on application to CCDC, 12 Union Road, Cambridge CB21EZ, U.K. (fax: (+44)1223–336–033; e-mail: deposit@ccdc.cam.ac.uk or http://www.ccdc.cam.ac.uk.

Acknowledgment. We gratefully acknowledge the financial support by the Deutsche Forschungsgemeinschaft and the Fonds der Chemischen Industrie.

Supporting Information Available: Crystallographic data for **6b** and **6d** as cif files and ^{1}H NMR spectra of polylactide samples (homodecoupled methine region). This material is available free of charge via the Internet at http://pubs.acs.org.

IC702312B

(31) Sheldrick, G. M. *SHELXL-97: A Program for Crystal Structure Refinement*; University of Göttingen: Göttingen, Germany, 1997.
(32) Farrugia, L. J. *J. Appl. Crystallogr.* **1999**, *32*, 837.